PROCEEDINGS OF SPIE REPRINT

SPIE—The International Society for Optical Engineering

Reprinted from

Photomask and Next-Generation Lithography Mask Technology VII

12–13 April 2000
Yokohama, Japan

Volume 4066

Structual and Thickness Distribution Evaluation of a Multi-Layer Photomask Blank with a X-Ray Reflectivity Method

Teruyoshi Hirano*[a], Hiroshi Wada[a], Masao Otaki[b], Ryuji Matsuo[c]
[a]Technical Research Institute, Toppan Printing Co.,Ltd., Sugito, Saitama 345-8508, Japan
[b]Asaka Plant, Toppan Printing Co.,Ltd., Niiza, Saitama 352-8562, Japan
[c]Rigaku Corporation, X-ray Research Laboratory, Akisima-shi, Tokyo, Japan 196-8666

ABSTRACT

The film thickness estimation is one of most important subject for the design up of photomask blank. To decrease the producing cost of silicon semiconductor chips, control photomask specifications and evaluate thickness technologies are the key technology. The grazing-incidence X-ray reflectivity method is very useful in order to measure thickness, density and interface roughness of photomask blank. In this paper, we report the adaptation of the X-ray reflectivity technology to photomask evaluation and prepare a thickness distribution map of mono- and multi-layer photomask blank.
A ZrSi oxide thin photomask blanks were prepared with DC sputtering method. The X-ray reflectivities of those photomask blanks were measured with RIGAKU ATX-E diffractometer system with asymmetric channelcut monochromater. The thicknesses maps of the photomask blanks were calculated with RIGAKU *XRR*° program. The *XRR*° calculations require model structures of the mono- and double-layer photomask blank. We estimated model structures of the films for better fitting between measured and calculated *XRR*° results. In the thickness distribution maps, the thickness were evaluated in Angstrom accuracy and a thickness difference between measurement positions were detected. The X-ray reflectivity method is a kind of high accuracy evaluation method of photomask blank thickness distribution map.

Keywords: Photomask Blank, Thickness, Thickness distribution, X-ray Reflectivity, Grazing-incidence

1. INTRODUCTION

In new technologies thin layered materials, for example PHOTOMASK BLANK, become increasingly important. Mono or multi-layer structures can be found in all kinds of research and development areas, like semiconductors, magnetic multi-layers, different coatings or optical applications. The photomask blank technologies are a kind of fine multi-layered film technologies in the field of electronics industries. The nano patterns printing technologies are developing day by day. The high quality, large size multi-layer film systems are required in the field of photomask blank. To decrease the production cost of silicon semiconductors chips, huge size photomasks are required. The in-plane thickness distribution, uniformity are very important for silicon chip production processes. For designing up large size high quality photomask blanks, the characterization technologies of nano scale thin film systems are important. Measurements of parameters like layer thickness, interface roughness, layer density and the description of originated inter layers are important for analyses, for development to control and production processes of the photomask blanks. The X-ray reflectivity method is a powerful non-destructive and very high accuracy measurement tool to characterize thin mono and multi-layer photomask blanks.

2. X-RAY REFLECTIVITY

The critical angle of external total reflection X-rays penetrate only a few nano-meters (typically 2 - 5 nm) into condensed materials. Above the critical angle the penetration depth increases rapidly. Grazing incidence X-ray reflectivity (GIXR) measurements are used to analyze sample surface and thin layers. The GIXR measurements allow to determine densities,

Correspondence: * Teruyoshi Hirano, Email: thirano@tri.toppan.co.jp; http://www.toppan.co.jp/; Telephone: +81-480-33-9054, FAX: +81-480-33-9022, ** Ryuji Matsuo, Email, r-matsuo@rigaku.co.jp; Telephone: +81-42-545-8139; FAX: +81-42-546-7090

In *Photomask and Next-Generation Lithography Mask Technology VII*, Hiroaki Morimoto, Editor, Proceedings of SPIE Vol. 4066 (2000) • 0277-786X/00/$15.00

thicknesses of layers on substrates and the roughness of external and internal interfaces. Provided the reflectivity is measured over a "wide" angler range (θ approximately 4 - 5°) and over at the least seven orders of magnitude in reflectivity, a minimum layer thickness in the order of 1 nm and density changes of about 1 - 2 % can be proven under optimal sample conditions.
The specular beam in the coherent approximation is simulated on the basis of Parratt's formalism for perfect structures [1]. The roughness of surface and internal interfaces is taken into account by developing the perturbation theory, namely distorted-wave Born approximation (DWBA) [2].

Reflectivity

The coherent scattering of the X-rays from the perfect multi-layer structure consisting of N layers can be calculated using well-known Fresnel-formulas for reflection coefficients r_j and transmission coefficients t_j,

$$r_{j,j+1} = \frac{k_j - k_{j+1}}{k_j + k_{j+1}} \qquad t_{j,j+1} = \frac{2k_j}{k_j + k_{j+1}} \qquad (1)$$

where k_j is z-component (we drop the index z) of the wavevectors in layer j, defined by the law of reflection as follow:

$$k_j = k_0 \sqrt{n_j^2 - \cos^2\theta_i}$$

k_0 is wavevector of incident wave and n_j is the reflective index of layer j, θ_i is the glancing angle of incidence. The Parratt's recursion equation are used to calculate the reflected intensity from the stack of layers,

$$X_j = e^{-2ik_j z_j} \frac{r_{j,j+1} + X_{j+1} e^{2ik_{j+1} z_j}}{1 + r_{j,j+1} X_{j+1} e^{2ik_{j+1} z_j}} \qquad (2)$$

where $X_j = R_j / T_j$ is the ratio of amplitudes R_j of the reflected and T_j of the transmitted waves within layer j and z_j is coordinate of j-interface between the layers j and j+1 [1,3].

Roughness

Since there are no perfect objects in the nature, the imperfection of the samples should be considered during the X-ray scattering process. The X-ray reflectivity takes into account the influence of rough surface and interface on X-ray reflectivity surveys. The conventional way to describe the effect of roughness is multiplication of the reflection coefficient by so-called static Debye-Waller factor [4].

$$\exp(-2k_j^2 \sigma_j^2) \qquad (3)$$

or by the factor introduced by Nevot and Croce [5].

$$\exp(-2k_j k_{j+1} \sigma_j^2) \qquad (4)$$

Here σ_j is the root-mean-square j-interface roughness. Every of these attenuation factors gives the better description of scattering process in different regions of incidence angle θ, the Debye-Waller form is applied far from the total external reflection (TER) region, whereas the Nevot-Croce form is more appropriate for the region of TER. The X-ray reflectivity utilizes the distorted-wave Born approximation (DWBA) approach to correct the Fresnel coefficients for the reflectivity and transmission [6].

$$\tilde{r}_{j,j+1} = r_{j,j+1} \exp\left[-2k_j k_{j+1}\sigma_j^2 - \frac{1}{2\pi^2} k_j k_0^2 \int \frac{d_{q_{//}}}{q_j} C(q_{//})\right]$$
$$\tilde{t}_{j,j+1} = t_{j,j+1} \exp\left[\frac{1}{2}(k_j - k_{j+1})2\sigma_j^2 - \frac{1}{4\pi^2}(k_j - k_{j+1})k_0 \int \frac{d_{q_{//}}}{q_j + q_{j+1}} C(q_{//})\right] \quad (5)$$

Here $C(q_{//})$ is the Fourier transform of the correlation function, and $q_j = (q_{//}, q_j)$ is the scattering vector with in-plane component $q_{//}$ within q_j within j-layer. The corrections (5) derived in the second-order DWBA tend to the formulas (3) and (4) in limiting cases and interpolate both forms of exponential coefficients in the intermediate region.

3. EXPERIMENTS

3.1. Preparation of mono-layer and multi-layer photomask blanks

The ZrSi oxide[7] mono-layer and multi-layer photomask blanks were used for the measurements. We prepared the photomask blanks with a DC sputtering method on a 6x6 inch quartz substrate. Table 1 shows deposition conditions of the mono- and double-layer photomask blanks. The mono-layer photomask blank (sample A) was prepared only a bottom layer of the double-layer photomask blank which preparation conditions are showed in the Table 1. The double-layer photomask blank (sample B) was made with the sputtering conditions shown in the Table 1. The film thickness of the samples were controlled by a film deposition time.

Table 1 Preparation conditions of the photomask blanks

Layer	Deposition time	Target	Gas composition (Volume ratio)	
top	224	ZrSi alloy	Ar / O_2	70 / 10
bottom	56	ZrSi alloy	Ar / O_2	70 / 1.5

3.2. X-ray reflectivity measurements

The X-ray reflectivity were measured with a high resolution diffractometer (ATX-E, RIGAKU). Figure 1 shows the optical configuration of the diffractometer for the measurements. The measurements of a reflectivity curves are performed using a coupled $\theta/2\theta$ scan. The X-ray source is a rotation target tube with copper anode. The experiments presented were

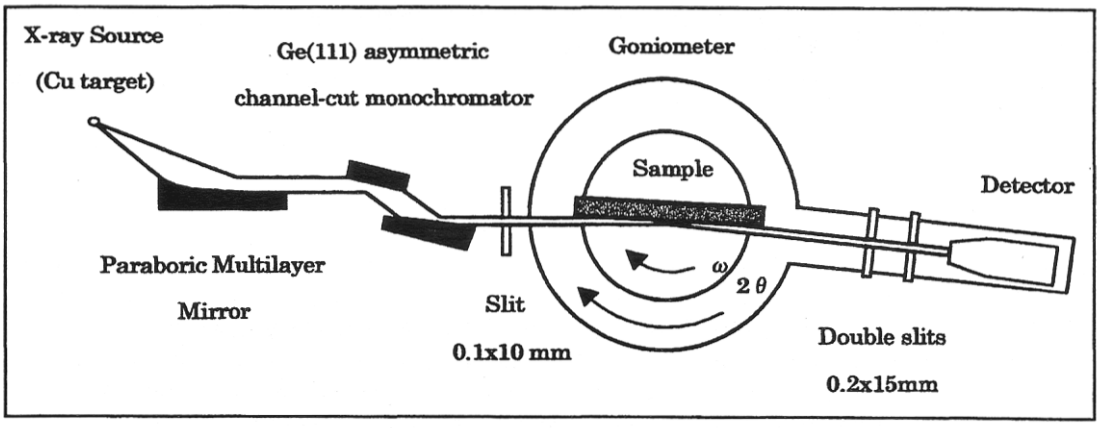

Fig. 1 The configuration of the experimental equipments for X-ray reflectivity measurements.

performed with a generator setting of 50 kV / 300 mA. The X-ray beam is concentrated by X-ray lens system. A Ge(111) asymmetric channelcut monochromator (2 crystals) was used for measurements.
An accurate calibration of the 2θ zero position and an accurate adjustment of the sample with respect to the incident beam should be done with an accuracy of approximately 0.001°. Since the dynamic range of the detector is limited a primary automatic attenuator is used at high intensities. This increases the dynamic intensity range to 9 decades. The X-ray reflectivity of the samples are measured in 0 - 8° (2θ).

Figure 2 shows the thickness measurement positions with the photomask blanks. The size of the measurement areas are about 10 x 15 mm^2 in all positions.

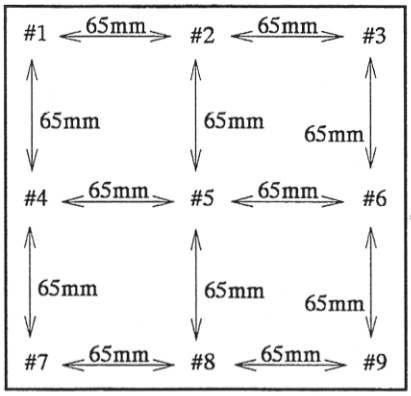

Fig.2 The position matrix of the measurement.

3.3. Evaluation of layer parameters

The information from the experimental data is extracted with the *XRR*° program system (RIGAKU). This program system simulates the theoretical X-ray reflectivity curves from the wide range of nano-structure mono- and multi-layer systems. The *XRR*° has the following advantages in comparing with previous analogous software systems.
- takes into account the diffuse scattering from rough surfaces and interfaces
- calculates the reflectivity curves from complex structures such as multi-layers and multi-groups superlattices
- considers the real experimental geometry
- works with the built-in extendable database of materials
- allow to fit the experimental data using modified Levenberg-Maequardt method for solution of nonlinear square problem
- proposes the friendly to user interface and graphics abilities

The validity of the program has been testified by fitting of real experimental data on X-ray scattering from different kinds of structures including semiconductor quantum wells, multi-layers, superlattice, amorphous thin films and other nano-structures.

All of calculations in this paper were carried out with *XRR*° program system on a Windows95 computer. We estimated layer parameters such as layer thickness, density and surface/interface roughness of the mono- and double-layer photomask blanks.

4. RESULTS AND DISCUSSIONS

4.1. The thickness map of the mono-layer photomask blank

4.1.1. Thickness evaluation by a mono-layer model

Figure 3 shows the comparison of the measured curve of the mono-layer photomask blank (sample A) and the calculated curve of it. In the Fig.3, we showed the calculated layer parameters. We executed the calculations with the mono-layer structure model. In the least-square processes of the parameters refinements, we use all of parameters example thickness

density and roughness of the layer model. In Fig.3, the coincidence between measured and calculated XRR° data is not fine in the initial region. We interpreted that the defect between the results measurement and calculation in the Fig.3 is important. Because the XRR° calculated density of the mono-layer photomask blank is very sensitive to the initial region of the measured XRR° data which is shown with the circle in the Fig.3.

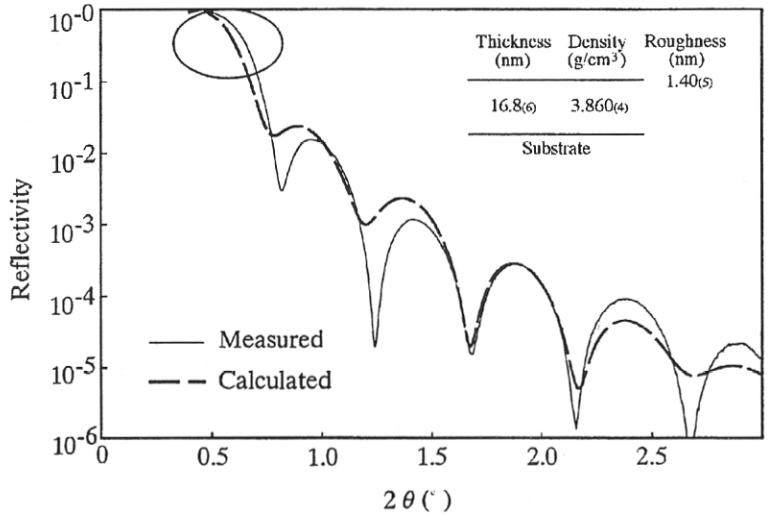

Fig.3 The measured and calculated X-ray reflectivity curves of mono-layer photomask blank (position #5).

Figure 4 shows the result of density refinement with the least-square processes in initial region. This result means that the high precision fitting of the density with the sample A. The coincidence between the measurement and calculation is very fine. The result shows the density of the sample A is 4.476(4) g/cm^3.

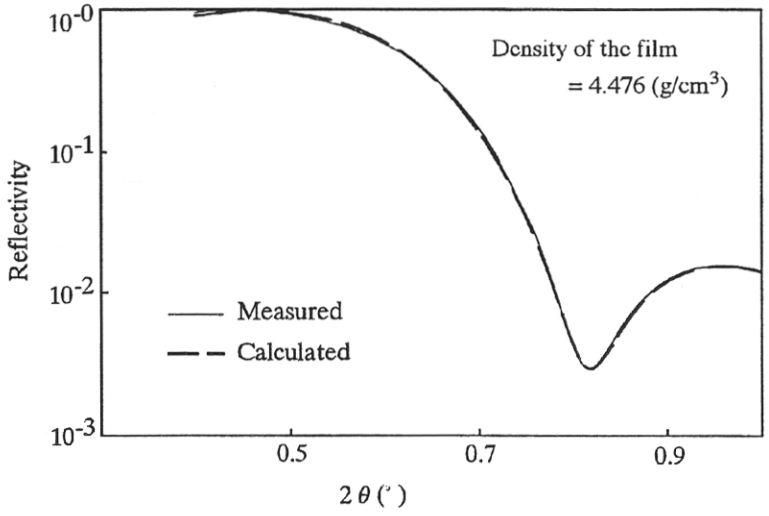

Fig.4 The measured and calculated X-ray reflectivity curves of mono-layer photomask blanks (position #5).

Figure 5 shows the measured and calculated results of sample A. In the Fig.5, we show the XRR° calculated layer parameters. On the fitting processes, the density of the film was fixed to 4.476 g/sm^3 refer to the result of Fig.4. The coincidence between the measurement and the XRR° calculation is better than the result in Fig.3. The calculated thicknesses 16.8((6) and 16.9(6) are almost equal each other. This result means that the value of the layer density have a little effect to the layer thickness for the thickness evaluation of photomask blank.

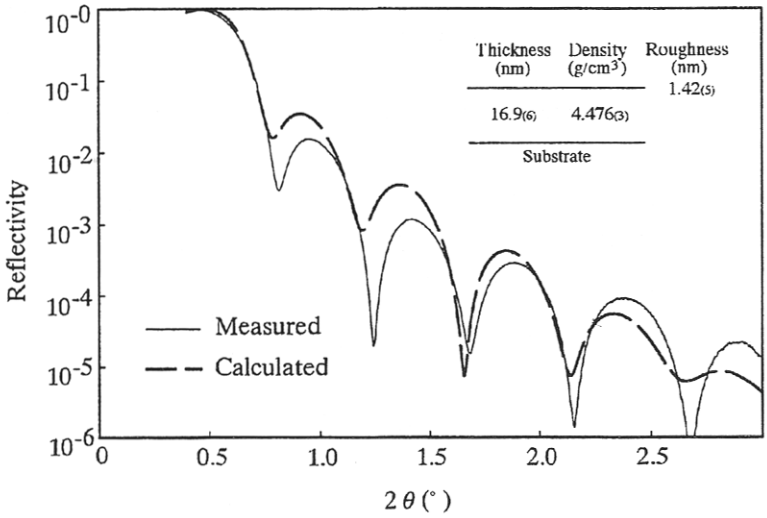

Fig.5 The measured and calculated X-ray reflectivity curves of mono-layer photomask blanks (position #5).

Table 2 shows that the XRR° calculated thickness map of the sample A based on the mono-layer model and fixed density. The thicknesses which were XRR° evaluations have high precision.

Table 2 Results of XRR° calculations of mono-layer photomask blank. The calculations were carried out with fixed film density to 4.476 g/cm3.

Measurement position	Thickness(S.D.) (nm)	Density(S.D.) (g/cm3)	Surface roughness(S.D.) (nm)
#1	17.2(6)	4.476(3)	1.41(5)
#2	17.3(6)	4.476(3)	1.43(5)
#3	17.3(7)	4.476(3)	1.44(6)
#4	17.2(6)	4.476(3)	1.44(5)
#5	16.9(6)	4.476(3)	1.42(5)
#6	16.9(6)	4.476(3)	1.44(5)
#7	16.9(6)	4.476(3)	1.44(5)
#8	16.9(6)	4.476(3)	1.55(5)
#9	16.9(6)	4.476(3)	1.44(5)

4.1.2. Thickness evaluation by a surface modified model

Figure 6 shows the comparison of the measurement curve and the calculated curve of the sample A. We think that all thin film objects have oxidized surface layer in the air[8]. For better fitting between the measurement and the calculation data, a modification of the model structure was needed. The modified model is shown in the Fig.6, the modified model has surface layer and core layer. The coincidence between the measured curve and calculated curve is fine. Table 3 shows the film parameters of the sample A. The calculated total film thickness of the position #5 is 16.80(7), this value is almost equal to the 16.9(6) such as calculated with simple layer model shown in Table 2. Only for film thickness evaluation, difference of the base models example mono-layer and three layers model is not so important for the calculations.

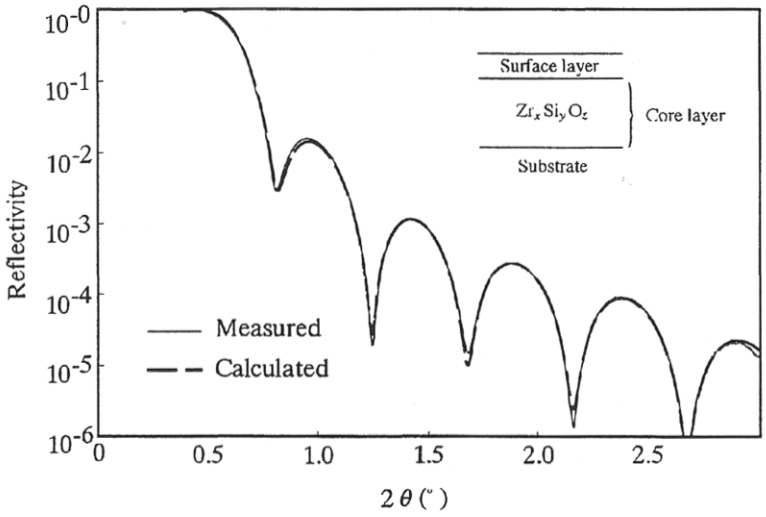

Fig.6 The measured and calculated XRR curves of mono-layer photomask blank (position #5).

Table 3 The film parameters of mono-layer photomask blank sample A. The evaluations were carried out with surface modified model.

Measurement position	Surface layer			Core layer		
	Thickness(S.D.) (nm)	Density(S.D.) (g/cm3)	Surface roughness(S.D.) (nm)	Thickness(S.D.) (nm)	Density(S.D.) (g/cm3)	Surface roughness(S.D.) (nm)
#1	1.45(1)	1.306(4)	0.678(3)	15.65(9)	4.290(4)	2.46(1)
#2	1.44(1)	1.268(4)	0.679(3)	15.74(8)	4.224(4)	2.43(1)
#3	1.33(1)	1.133(4)	0.648(3)	15.91(9)	4.268(4)	2.48(1)
#4	1.58(1)	1.295(4)	0.719(4)	15.44(9)	4.290(4)	2.48(1)
#5	1.57(1)	1.275(4)	0.710(3)	15.23(6)	4.281(4)	2.40(1)
#6	1.61(1)	1.250(4)	0.689(2)	15.18(5)	4.284(4)	2.35(1)
#7	1.60(1)	1.294(4)	0.750(3)	15.24(7)	4.248(4)	2.44(1)
#8	1.69(1)	1.355(4)	0.973(3)	15.17(5)	4.242(4)	2.39(1)
#9	1.62(1)	1.311(4)	0.709(2)	15.21(5)	4.283(4)	2.33(1)

4.2. The thickness map of the double-layer photomask blanks
4.2.1. Optimum model for thickness evaluation with sample B

The coincidence between measured and XRR° calculated curves is depends on the defined model structure of sample film. For high accuracy evaluation of thickness with a photomask blank, the model structure of the film for XRR° fitting process is important. Figure 7 shows the measured curve (measured position is #5) and calculated it is based on double-layer model. Also, the layer model which used for XRR° calculation is shown in the Fig.7. The coincidence between measured and calculated curves is not good. It is clear that more multiple layer model required for better fitting between measured and calculated.

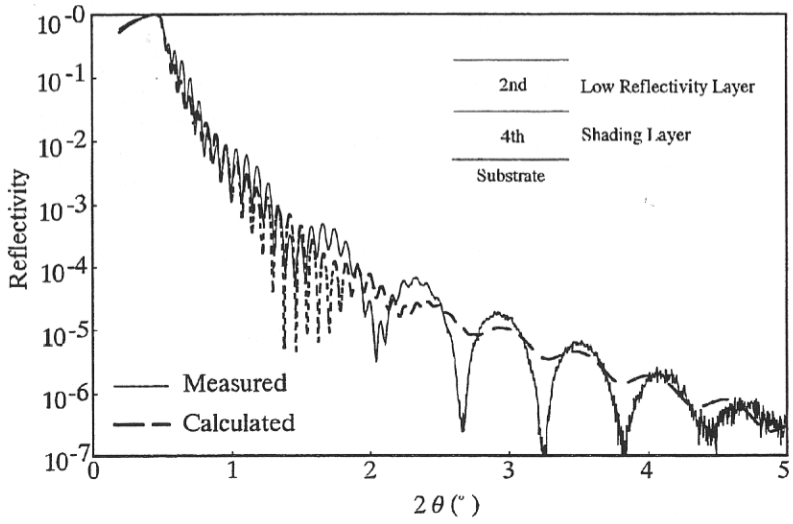

Fig.7 The measured and calculated XRR° curves of double-layer photomask blank (position #5). Calculation model is shown in the Fig.

Figure 8, Figure 9 and Figure 10 show the measured XRR° curves (measured position is #5) and XRR° calculated curves which are based on multiple layer models respectively. Those defined structure models are shown in the Fig.8 ~ Fig.10 respectively. Estimated XRR° calculations used with multiple layer model are fine fitted to measured curves. The 5 layer

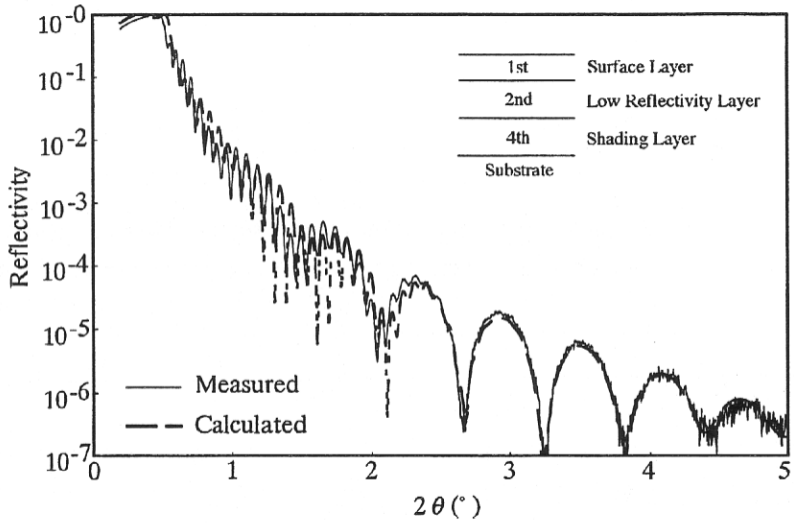

Fig.8 The measured and calculated XRR° curves of double-layer photomask blank (position #5). Calculation model is shown in the Fig.

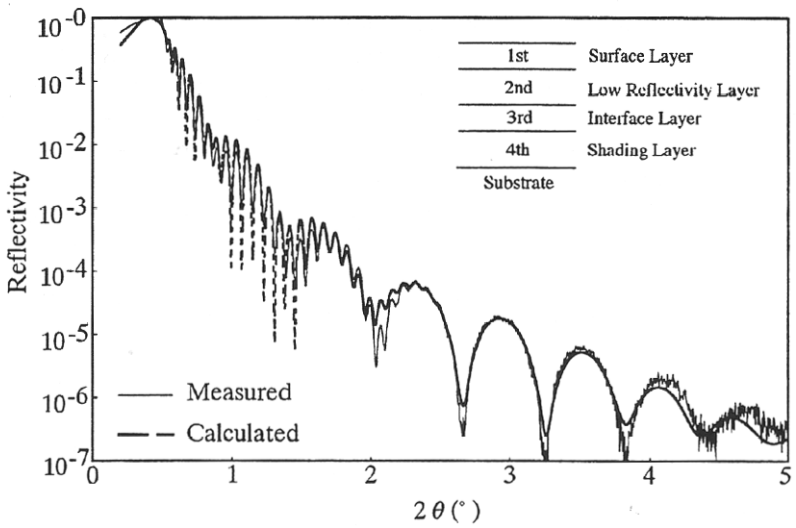

Fig.9 The measured and calculated XRR curves of double-layer photomask blank (position #5). Calculation model is shown in the Fig.

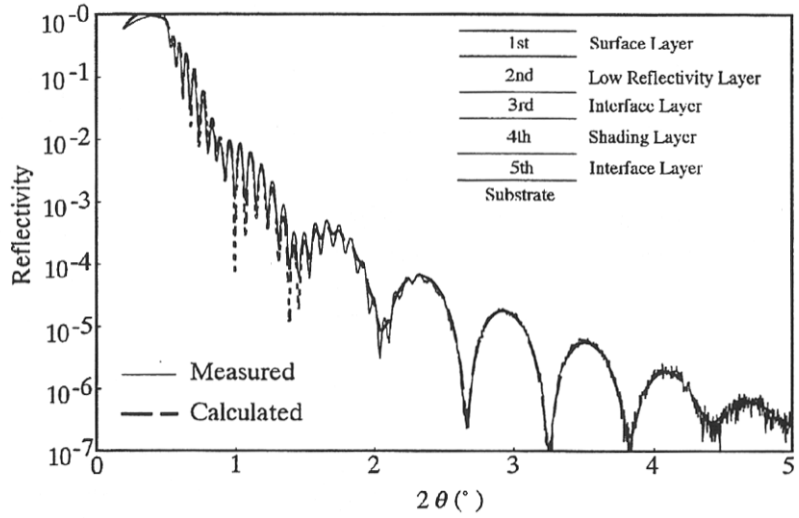

Fig.10 The measured and calculated XRR curves of double-layer photomask blank (position #5). Calculation model is shown in the Fig.

Table 3 The calculated layer thicknesses with some multiple layer models

Base model	Layer Thickness (S.D.) (nm)					Total Thickness (S.D.) (nm)
	1st	2nd	3rd	4th	5th	
2 layers model		86.2(3.0)		16.6(5)		102.7(3.5)
3 layers model	0.0(0)	88.4(1.6)		15.2(3)		103.6(1.9)
4 layers model	0.0(0)	86.5(1.5)	2.49(4)	13.9(2)		102.9(1.7)
5 layers model	0.0(0)	87.0(1.0)	2.58(3)	13.2(2)	0.84(1)	103.6(1.2)

model shown in the Fig.10 is best fitted to the measured curve. Table 3 shows the estimated layer thicknesses in each models. The result based on 5 layer model is most small standard deviation in the thickness. We selected 5 layer model for the thickness map calculation.

4.2.2. Thickness map of double-layer photomask blank

Table 4 shows the measured thickness map of the double-layer photomask blank sample B. The evaluated thicknesses are calculated in Angstrom accuracy. In those results, the measured thickness values are divided to 3 groups as #1 ~ #3, #4 ~ #6 and #7 ~ #9. On these results, position #7, #8 and #9 are slightly thinner than #1 ~ #6 positions. In preparation process, the substrate was moved along #1 ~ #3 direction. This result indicates that the deference between #7 ~ #9 and #1 ~ #3, #4 ~ #6 is owing to the deference of sputter condition for film deposition process.

Table 4 Evaluated thickness distribution map of the double-layer photomask blank sample B

Measurment position	Layer thickness (S.D.) (nm)					Total thickness (S.D.) (nm)
	1st	2nd	3rd	4th	5th	
#1	0.0(-)	87.2(1.3)	0.48(1)	12.6(2)	1.26(2)	101.5(1.5)
#2	0.0(-)	85.4(1.2)	1.98(3)	13.8(2)	0.81(1)	102.0(1.4)
#3	0.0(-)	84.8(1.1)	2.20(3)	13.8(2)	0.82(1)	101.6(1.3)
#4	0.0(-)	85.6(1.3)	4.15(6)	13.1(2)	0.79(1)	103.6(1.6)
#5	0.0(-)	87.0(1.0)	2.58(3)	13.2(2)	0.84(1)	103.6(1.2)
#6	0.0(-)	87.1(1.1)	2.35(3)	13.2(2)	0.87(1)	103.5(1.3)
#7	0.0(-)	86.9(1.1)	0.0(-)	13.6(2)	0.0(-)	100.5(1.3)
#8	0.0(-)	87.0(1.0)	0.0(-)	13.4(2)	0.59(1)	101.0(1.2)
#9	0.0(-)	86.2(1.0)	0.0(-)	13.6(2)	0.65(1)	100.5(1.2)

5. CONCLUSIONS

The X-ray reflectivity measurements were performed with mono- and multi-layer PHOTOMASK BLANK. Some photomask blanks and component layers of them were prepared for evaluations of those layer parameters. The model film structures for high accuravy **XRR**° calculations were dfined. The high accuracy thickness maps of the mono- and multi-layer photomask blanks were made by high resolution X-ray reflectivity measurements and **XRR**° program system with least-square processes. The calculated thickness by the **XRR**° with X-ray reflectivity results have high accuracy and precision. The layer thickness maps of the mono- and multi-layer photomask blank were plesented. These thickness maps are very important to design and product out a high quiality photoamsk blank. The **XRR**° method is a new technology for improvement a highly efficient photomask blank.

6. REFERENCES

1. L.G.Parratt, "Surface Studies of Solids by Total Reflection of X-rays", *Phys. Rev. B* **95**, pp. 359-369, 1954.
2. S.K.Sinha, E.B.Sirota, S.Garoff and H.B.Stanley, "X-ray and neutron scattering from rough surfaces", *Phys.Rev.B* **38**, pp. 2297-2311, 1988.
3. J.-P.Schlomka, M.Tolan, L.Schwalowsky, O.H.Seeck, J.Stettner and W.Press, "X-ray diffraction from Si/Ge layers: Diffuse scattering in the region of total external reflection", *Phys.Rev.B* **51**, pp. 2311-2321, 1995.

4. P.Beckman and A.Spizzichino, *The Scattering of electromagnetic Waves from Rough Surfaces* (Pergmon, Oxford, 1963)
5. L.Névot and P.Croce, "Caractérisation des surfaces par réflexion rasante de rayons X. Application à l'étude du polissage de quelques verres silicates", *Rev.Phys.Appl.* **15**, pp. 761-779 1980.
6. D.K.G.de Boer, "Influence of the roughness profile on the specular reflectivity of x rays and neutrons", *Phys.Rev.B* **49**, pp. 5817-5820, 1994.
7. N.Fukuhara, T.Haraguchi, K.Kanayama, T.Matsuo, Y.Hattori, T.Ohshima and M.Otaki, "Development of ZrSiO attenuated phase-shift mask for ArF excimer laser lithography", *Part of the 19th Annual BACUS Symposium on Photomask Technology, Monterey, California, Proceedings of SPIE*, **Vol.3873**, pp. 979-986 1999.
8. T. Hirano, R. Matsuo, K. Tomiyama, I. Yazawa, H. Wada, M. Otaki and K. Omote, "HIGH RESOLUTION THICKNESS MEASUREMENTS AND EVALUATION OF A PHOTOMASK BLANK", *Part of the 19th Annual BACUS Symposium on Photomask Technology, Monterey, California, Proceedings of SPIE*, **Vol.3873**, pp. 562-572 1999.